Journal of Engineering Mathematics **49:** 339–358, 2004.

Optimal control of polymer morphologies

MARTIN BURGER, VINCENZO CAPASSO[1] and ALESSANDRA MICHELETTI[1]
Industrial Mathematics Institute, University Linz, Altenbergerstr. 69, 4040 Linz, Austria (E-mail: martin.burger@jku.at; [1]*Milan Research Centre for Industrial and Applied Mathematics, Università di Milano, Via Saldini 50, 20133 Milano, Italy (E-mails: Vincenzo.Capasso@mat.unimi.it; Alessandra.Micheletti@mat.unimi.it)*

Received 7 May 2002; accepted in revised form 18 December 2003

Abstract. This paper is devoted to the optimal design of polymeric materials through control of the cooling during the crystallization process. The optimality is defined in terms of optimal mechanical properties, which are directly related to the morphology of the solidified polymeric material. As a characterizing mathematical entity to be controlled the contact interface density is introduced and its relations to other structure variables such as temperature and crystallinity is discussed. Not only a general optimal control approach is presented, but also some relevant special cases are discussed, for which a more detailed analysis can be carried out. It is shown that under reasonable conditions on the parameters and the process, these optimal-control problems have solutions in appropriate function spaces and the optimality conditions derived from the Lagrangian formulation are discussed. Finally, the numerical approximation is discussed and results for some test examples are presented.

Key words: contact interfaces, crystallization, morphology, optimal cooling

1. Introduction

Crystallization processes play a fundamental role in structure development and material processing for many types of materials such as polymers or steel. In general, crystallization is modeled as a birth-and-growth process, consisting of the *birth* of crystals (nucleation), which is a stochastic process in time and space, and their *growth*, which is usually modeled in a deterministic way. Over the last years and decades, much research has been concerned with the mathematical description of such processes in order to obtain insight into the structure formation during solidification. The common idea of most approaches is the meso- or macroscopic description of the process by mean quantities, which are derived as averages or expected values of the corresponding (stochastic) microscopic quantities.

Obviously, such a modeling procedure heavily relies on the understanding of nucleation and growth on the microscale as well as on the determination of important material parameters, which is a difficult task in practice. *Polymers* are a class of materials, where these subprocesses seem to be well-understood (*cf.* [1] for a comprehensive overview) and where material parameters can be determined, either in direct or in indirect ways by parameter identification techniques (*cf.*, *e.g.*, [2–5]). Therefore, mathematical models for structure formation have been used in this area with particular success. The usual structure variables used for the macroscopic description of non-isothermal crystallization are the *temperature* θ and *degree of crystallinity* ξ, as functions of space and time. The degree of crystallinity $\xi(x,t)$ represents the probability that a point x belongs to the crystalline phase Θ^t at time t; it can be interpreted equivalently as the expected value of the indicator function of the crystalline phase. We will review the basic models for the evolution of these structure variables in Section 2.

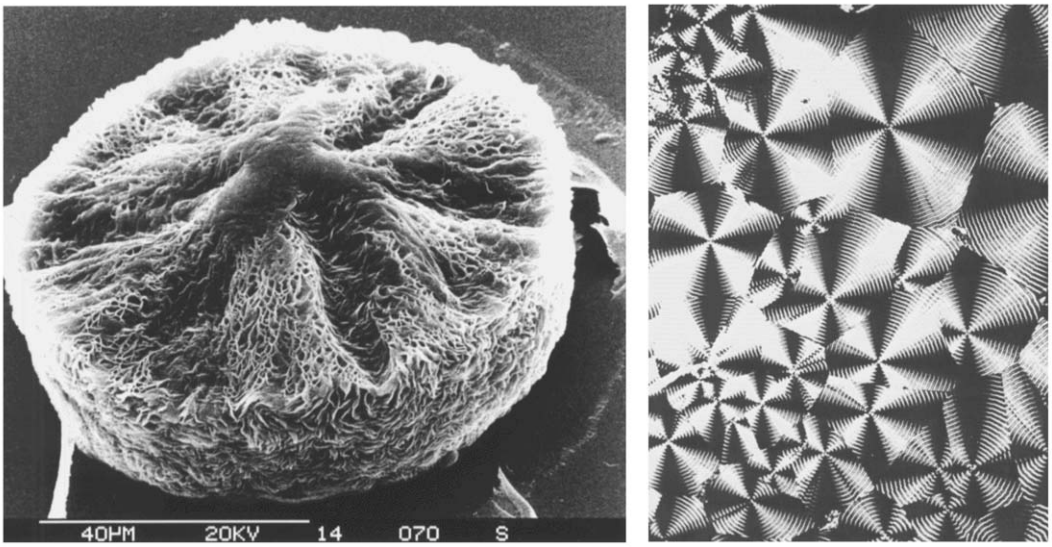

Figure 1. A polymeric crystal grown in a 2D experiment (above) and the final morphology (right, both obtained with isotactic Polypropylene).

In industrial applications, models for non-isothermal crystallization are not only used to obtain further insight into the process, but also for predicting mechanical properties of the final product. As we will see in Section 1.1, these properties are mainly related to the morphology (in particular to the distribution of grain sizes, *cf.* [6, 7]) of the final crystalline structure, which is illustrated in Figure 1. Therefore, it seems to be a natural next step to control the crystallization process in such a way that the final morphology is optimal with respect to some suitable criterion. The physical quantity that can be controlled in the easiest way is the cooling rate at the boundary of the sample. In this paper we shall develop a mathematical framework for such an optimal-control approach and investigate the structure of solutions from an analytical, as well as a numerical point of view.

This paper is organized as follows: in Section 1.1 we discuss typical industrial needs for polymeric materials and their implication for an "optimal structure". In Section 2 we recall some basic models for crystallization and the interaction with heat transfer, with a special focus on *morphological state variables* in Section 2.1. There we also introduce the *density of contact interfaces*, which serves as a mathematical model for the grain-structure of the crystalline morphology. In Section 3 we set up a general optimal control problem for polymer crystallization processes, special cases of which are discussed in Section 4. The final Sections 5 and 6 are devoted to a detailed discussion of the spatially homogeneous case and some numerical experiments related to the arising optimal-control problem.

1.1. Industrial processing and optimal structures

Under industrial processing conditions, the aim is to produce homogeneous material structures with good mechanical properties. Since the *yield stress* σ_γ of the crystallized material is related to the average grain diameter d via the so-called *Hall-Petch relation* (*cf., e.g.,* [8])

$$\sigma_\gamma = K d^{-\frac{1}{2}} + \sigma_0, \tag{1.1}$$

where K is a positive constant and σ_0 is a constant offset; optimal mechanical properties are directly related to optimal morphological properties. The optimality criterion for the crystalline morphology is a fine-grained structure, which is close to spatial homogeneity. In practice, the latter can be realized only on a meso- or macroscale, *i.e.*; local averages over appropriate sets (in the same way as for the crystallinity ξ) should be homogeneous. In Section 3, we will develop a mathematical model for these phenomenological criteria, leading to a cost functional that incorporates a pay-off between small grain sizes and spatial homogeneity of a relevant morphological state variable, namely the contact interface density.

The design quantity under industrial processing conditions is the temperature q at the boundary of the sample, which can be realized by an appropriate cooling strategy, the speed of cooling is limited for physical and technological reasons and therefore we have a constraint of the form

$$-a \leq \frac{\partial q}{\partial t} \leq 0, \qquad \text{a.e. on } \partial\Omega \times (0, S), \tag{1.2}$$

with some constant $a > 0$. In addition, it is necessary that a certain degree of crystallinity is achieved at the final time S, which causes a second constraint of the form

$$\xi(x, S) \geq 1 - b, \qquad \text{a.e. in } \Omega, \tag{1.3}$$

with a small constant $b > 0$. Obviously, these two restrictions can be satisfied only if the final time S is not too small (since a limited speed of cooling also implies limits for nucleation and growth), but this is usually guaranteed from previous experiments.

We want to mention that an optimization of the morphological structure for fixed final time S might not be the only interesting approach for the optimization of industrial processing. An important problem for efficient manufacturing would be to minimize the processing time S, with some restrictions on cooling, final crystallinity and on the final morphology. Such approaches to optimal processing are, however, beyond the scope of this paper and will therefore be left to future research.

2. Models for crystallization and heat transfer

On a microscopic scale, a crystallization process can be described by the sets Θ_j^t, $j = 1, \ldots, N$, which denote the individual crystals at time $t > 0$. To each crystal, a nucleation event $(X_j, T_j) \in \Omega \times \mathbb{R}_+$ is associated, which consists of a random variable T_j for the time of the nucleation and a random variable X_j for the location. Under the usual conditions, the nucleation process can be modeled as an inhomogeneous Poisson process in space and time (*cf.* [9, 10]), and a reasonable model for the nucleation rate α is given by

$$\alpha(x, t) = \dot{N}(T(x, t)) + \frac{\partial}{\partial t}\widetilde{N}(T(x, t)), \tag{2.1}$$

with appropriate material functions $\dot{N}$ and $\widetilde{N}$, depending on the temperature T (*cf.* [11]). For typical polymeric materials and temperature regimes, the second term is dominating and therefore it is assumed that $\dot{N} \equiv 0$, which will also be done in the remainder of the paper. Once nucleated, a crystal grows in a normal direction with growth rate g, whose dependence upon the space variable x and time t is due to its dependence upon the underlying temperature field (*cf.* [11, 12, 4])

$$g(x, t) = G(T(x, t)). \tag{2.2}$$

Thus, heat transfer in the material is the driving force of the crystallization process (via nucleation and growth); but *vice versa* it is influenced by the solidification process via the latent heat L released during the moment of phase change. A mathematical model for the heat transfer process is given by (*cf.* [13, 9])

$$\frac{\partial T}{\partial t} = D\Delta T + L\frac{\partial}{\partial t} I_{\Theta^t}, \tag{2.3}$$

where I_{Θ^t} is the indicator function of the crystalline phase $\Theta^t = \bigcup \Theta_j^t$. Note that this heat-transfer model coupled to the growth of crystals can also be interpreted as a moving-boundary problem in Θ^t and $\Omega - \Theta^t$, with appropriate conditions at the interface between the phases (*cf.* [14] for further details).

For typical polymeric materials, a crystallization process involves three natural scales (*cf.* [13, 9]):

- A *microscale* at which the growth of crystals occur (note that G is rather small in general).
- A *mesoscale*, at which we may consider the crystals to be numerous, but still small to a typical size for temperature.
- A *macroscale* corresponding to the heat-transfer process.

On a macroscopic scale, the crystallization is usually described by corresponding averaged values, *i.e.*,

$$\xi(x,t) := E\left[I_{\Theta^t}(x)\right], \qquad \theta(x,t) := E\left[T(x,t)\right]. \tag{2.4}$$

The function ξ is called degree of crystallinity; it coincides with the probability that the point x is covered by the crystalline phase at time t. In [9], a coupled system of random differential equations for the stochastic quantities I_{Θ^t}, T together with the metric surface density u_{stoch} and the oriented surface density v_{stoch} has been derived. By a heuristic "law of large numbers" an associated hybrid model describing the evolution of θ, ξ and the mean free surface densities u and v, has been deduced:

$$\frac{\partial \theta}{\partial t} = D\Delta\theta + L\frac{\partial \xi}{\partial t} \tag{2.5}$$

$$\frac{\partial \xi}{\partial t} = G(\theta)(1-\xi)u \tag{2.6}$$

$$\frac{\partial u}{\partial t} = \operatorname{div}\left(G(\theta)v\right) + \mathcal{F}_d(\widetilde{N}, G, \theta), \tag{2.7}$$

$$\frac{\partial v}{\partial t} = \nabla(G(\theta)u), \tag{2.8}$$

where $\mathcal{F}_d$ is a dimension-dependent source term, given by

$$\mathcal{F}_2(\widetilde{N}, G, \theta) = 2\pi G(\theta)\widetilde{N}(\theta), \tag{2.9}$$

for $\Omega \subset \mathbb{R}^2$, and by

$$\mathcal{F}_3(\widetilde{N}, G, \theta) = 4\pi G(\theta)\int_0^t G(\theta)\widetilde{N}(\theta)\,\mathrm{d}s, \tag{2.10}$$

for $\Omega \subset \mathbb{R}^3$. We will focus on the case $d = 2$ in the following, but we want to mention that analogous reasoning is possible for $d = 3$, too.

The above system of differential equations is usually supplemented by the initial values

$$\theta = \theta_0, \qquad \xi = u = 0, \qquad v = 0, \tag{2.11}$$

at $t = 0$, and by the boundary conditions

$$\frac{\partial \theta}{\partial \nu} + \beta(\theta - q) = 0 \tag{2.12}$$

$$u + v.\nu = 0 \tag{2.13}$$

on $\partial\Omega \times \mathbb{R}_+$, where ν is the unit outer normal vector. For the sake of simplicity we consider the case of a very large heat-transfer coefficient β, which allows to approximate the Robin-type boundary condition (2.12) by

$$\theta = q \qquad \text{on } \partial\Omega \times \mathbb{R}_+. \tag{2.14}$$

2.1. Morphological state variables

In order to predict the material properties of a solidified sample, also other structure variables are needed, which are usually called *morphological state variables*. A fundamental morphological state variable is the crystal density $\Lambda(x, t)$, which represents the density of the expected number of crystals per unit of volume; the evolution of this density can be computed from the knowledge of the degree of crystallinity and the nucleation rate only, via

$$\Lambda(x, t) = \int_0^t (1 - \xi(x, s))\alpha(x, s)\, \mathrm{d}s. \tag{2.15}$$

where α denotes the nucleation rate. The distribution Λ gives the number of crystals per unit of volume, i.e., for a set $A \subset \Omega$, the quantity

$$N_t(A) := \int_A \Lambda(x, t)\, \mathrm{d}x$$

gives the expected number of crystals in S at time t, which is a good approximation to the real number of crystals in S if the set is of meso- or macroscopic size.

Another important quantity is the *contact-interface density* γ, which represents the spatial distribution of contact interfaces between distinct crystals and is of particular importance for the prediction of the mechanical properties of the solidified material. In the special case of spherulitic crystallization, which corresponds to isothermal experiments, there exists a well-developed theory (*cf.* [15–19]), which heavily uses the spatial invariance of the contact-interface density. In the general case of spatially heterogeneous nucleation and growth, which is the case in non-isothermal crystallization, this property does not hold, and therefore a localized theory for the contact-interface density is needed. Such a local approach has been introduced recently by the authors (*cf.* [20, 21]), and is based on *local spherical distributions*, a well-studied concept in stochastic geometry. More precisely, the local density of contact interfaces, denoted by $\gamma(x, t)$, is defined via

$$\gamma(x, t) = \lim_{r \downarrow 0} \frac{E[\mu^n(\Xi_n^t \cap B_r(x)]}{\mu^d(B_r(x))}, \tag{2.16}$$

where Ξ_n^t denotes the (random) set of all contact interfaces of Hausdorff dimension n (equal to 1 for $d = 2$, and 2 for $d = 3$). For $\Omega \subset \mathbb{R}^d$, $d \geq 2$ it has been shown (*cf.* [21]) that γ is related to the mean free surface density u and the degree of crystallinity ξ via the differential equation

$$\frac{\partial \gamma}{\partial t} = c_d g(1-\xi)u^2, \qquad \gamma|_{t=0} = 0, \tag{2.17}$$

where c_d is a dimension-dependent constant, and g is the growth rate (as above). For the sake of simplicity we rescale γ such that $c_d = 1$ in the following.

The contact-interface density is directly related to the grain structure of the material, since a high value of γ indicates many small crystals, whereas a small value indicates few interfaces and therefore either few or rather large crystals. Moreover, if γ is close to a constant distribution in Ω, we may expect a uniform structure of the material. We finally mention that also the quantity Λ could be used as an indicator for the crystalline structure in principle, but since it is a density for the distribution of the crystals only, we have to expect that it contains much less information about the grain sizes. Therefore, we will use the contact-interface density as the main morphological variable to be incorporated into an optimization criterion in the following section.

3. Optimal cooling strategies

In this section we will set up a control problem that can be used for optimizing the crystalline structure of the final sample. Since we can only control the temperature at the boundary, our main task is then to find an optimal cooling strategy, with the restrictions introduced in Section 1.1. We start with the construction of an appropriate cost functional.

3.1. Cost functional

The discussion in the previous sections shows that a cost functional to be minimized in order to obtain an optimal morphology should consist of three parts: a first one corresponding to the aim of "many, small crystals", a second one corresponding to the aim of spatial uniformity and a third one to keep the cooling strategy as close as possible to an *a-priori* strategy q^*, which can represent *e.g.* the cooling strategy used so far. This combination is realized via the cost functional

$$C(\gamma, q) := -\int_\Omega \gamma(x, S)\, \mathrm{d}x + \frac{\kappa}{2}\int_\Omega |\nabla \gamma(x, S)|^2\, \mathrm{d}x + \eta D(q - q^*). \tag{3.1}$$

Clearly, the first term corresponds to the goal of maximizing the contact-interface density in Ω and the second term to the goal of minimizing the variation of γ with respect to the spatial variable. The penalty parameter κ accounts for the pay-off between these two terms: a large value of $\kappa \in \mathbb{R}_+$ causes the second goal to dominate, while a small value means that mainly the total surface of the contact interfaces in Ω is maximized. The third term D can be chosen, *e.g.*, as the square of a norm or seminorm on the space of controls q; we will present some interesting examples in Section 4. An alternative to the cost functional (3.1) is given by

$$C_p(\gamma, q) := -\int_\Omega \gamma(x, S)\, \mathrm{d}x + \frac{\kappa}{p}\int_\Omega |\nabla \gamma(x, S)|^p\, \mathrm{d}x + \eta D(q - q^*), \tag{3.2}$$

with $1 \leq p < \infty$, which causes a slightly different structure of the optimal distribution γ. For instance, in the case of $p = 1$, it is well-known that the second term in (3.2) favors piecewise constant functions γ as optimal solutions.

From a mathematical point of view, the cost functional C defined by (3.1) is well-defined for $\gamma \in C([0, S]; H^1(\Omega))$, where we use the Soboloev space $H^1(\Omega) = W^{1,2}(\Omega)$ (*cf., e.g.*, [22] for an overview of Sobolev spaces and [23] for general notation). The modified cost functional C_p from (3.2) is well-defined on the space $C([0, S]; L^p(\Omega))$, but not convex in general. However, the convexity of the cost functional does not ensure the convexity of the optimal-control problem arising when the minimization of the cost is coupled to the evolution equations for γ, which may introduce non-convexity to the problem due to their nonlinear structure.

3.2. State and control variables

As noticed above, the optimal control of the morphology consists of minimizing the functional C defined in (3.1), supplemented by the constraints introduced by the underlying state equations (2.5–2.8) and (2.17), the initial and boundary conditions eqrefinitialc, (2.13), (2.14), as well as by the technological constraints (1.2), (1.3).

As is usual for optimal-control problems, we can split the quantities arising in the problems into the *state variables* $(\gamma, \xi, u, v, \theta)$ and the *control variable* q. Appropriate function spaces for the state variables depend on the analysis of the state equations, which is not available in the most general case, so far. In some particular case, this analysis can be carried out and will therefore be presented in Section 4.

A minimal demand on the choice of function spaces for the state is that the cost functional and the terms involved in the additional constraints are well-defined on these spaces. This implies in particular $\gamma \in C(0, S; H^1(\Omega))$ as noticed above and the constraint (1.3) makes a choice like

$$\xi \in H^1(0, S; L^2(\Omega))$$

favorable.

Summing up, we have to solve the minimization problem

$$C(\gamma, q) \to \min_{(\gamma,q)\in V\times \mathcal{Q}_{ad}} . \tag{3.3}$$

In the following sections we will discuss some limiting cases for the crystallization process, which clarify different aspects of the morphology control problem.

4. Special cases

In this section, we will investigate some special cases of the crystallization model obtained, either as scaling limits or for simple geometric situations. We start with the spatially homogeneous case, where the cost functional reduces to the first (linear) term and an optimal-control strategy consists of maximizing the total surface of the contacts, since the resulting interface density is spatially homogeneous anyway. The second special case arises for constant growth rate, which is a limit for materials where the temperature variance of the nucleation rate dominates the one of the growth rate; it clarifies the coupling between hyperbolic and

parabolic parts of the model. Finally, we investigate the control in the generalized Avrami-Kolmogorov model, which can be interpreted as a scaling limit. There the model reduces to an integro-differential equation for the temperature and we obtain a control problem of parabolic type.

4.1. SPATIAL HOMOGENEITY

In certain applications one must deal with crystallization in a sample with very small height, *i.e.*, in a domain of the form $\Omega \times [0, h]$, with $h \ll 1$ and $\Omega \subset \mathbb{R}^3$, with strong cooling on bottom and top of the sample (*i.e.*, in $\Omega \times \{0\}$ and $\Omega \times \{h\}$). In this case it is reasonable to use the two-dimensional crystallization model, but the heat-transfer model changes to

$$\frac{\partial \theta}{\partial t} = \beta(\theta - q) + K\frac{\partial \xi}{\partial t}, \tag{4.1}$$

with appropriate constants β and K, and q is the outside temperature (cf. [24] for further details).

If q is homogenous in space, which is the typical case in such applications, the crystallization and heat-transfer model admits a spatially homogenous solution and, as a consequence, also the contact interface density γ is homogeneous with respect to space. Hence, we obtain the simplified optimal-control problem (with $\eta = 0$)

$$C(\gamma)|\Omega|^{-1} = \gamma(S) \to \min_{\gamma}, \tag{4.2}$$

subject to the equality constraints

$$\frac{\partial \gamma}{\partial t} = G(\theta)(1 - \xi)u^2, \qquad \gamma(0) = 0, \tag{4.3}$$

$$\frac{\partial \xi}{\partial t} = G(\theta)(1 - \xi)u, \qquad \xi(0) = 0, \tag{4.4}$$

$$\frac{\partial u}{\partial t} = F(\theta), \qquad u(0) = 0. \tag{4.5}$$

$$\frac{\partial \theta}{\partial t} = \beta(\theta - q) + K\frac{\partial \xi}{\partial t}, \qquad \theta(0) = \theta_0, \tag{4.6}$$

where $F(\theta) := 2\pi G(\theta)\widetilde{N}(\theta)$, and the inequality constraints

$$-a \le \tfrac{\partial q}{\partial t}(t) \le 0, \qquad \forall\, t \in [0, S], \tag{4.7}$$

$$\xi(S) \ge 1 - b. \tag{4.8}$$

The set of admissible controls is given by

$$Q_{ad} := \big\{ q \in C([0, S]) \mid q(0) = \theta_0,\, q \text{ is piecewise } C^1 \text{ on } [0, S], \text{ and satisfies (4.7)} \big\}. \tag{4.9}$$

Thus, in this case we obtain a state-constrained optimal-control problem for a system of ordinary differential equations, the cost functional is linear. A detailed analysis and solution methods for this problem will be presented in Section 5.

4.2. AVERAGED GROWTH

For some polymeric materials, the nucleation rate $\widetilde{N}$ is much more sensitive to temperature variation than the growth rate G and dominates the process. In this case, the growth rate can be approximated by a constant average value, without restriction of generality we assume that $G \equiv 1$. If we introduce the new variable φ satisfying

$$\frac{\partial \varphi}{\partial t} = u, \qquad \varphi(0) = 0, \tag{4.10}$$

then the functions (ξ, u, v) can be eliminated from the crystallization model, since they are determined from φ by the relations

$$\xi(x,t) = 1 - \mathrm{e}^{-\varphi(x,t)}, \quad u(x,t) = \frac{\partial \phi}{\partial t}(x,t), \quad v(x,t) = \nabla \varphi(x,t). \tag{4.11}$$

We want to mention that φ has the physical meaning of a *mean free volume density* of the crystals grown in the absence of impingement (*cf.* [13, 11] for further details).

With the new variable φ, the crystallization model can be transformed to a wave equation with temperature dependent source, i.e.,

$$\frac{\partial^2 \varphi}{\partial t^2} = \Delta \varphi + F(\theta), \qquad \varphi|_{t=0} = 0, \tag{4.12}$$

in $\Omega \times (0, S)$, with the boundary condition

$$\frac{\partial \varphi}{\partial t} + \frac{\partial \varphi}{\partial \nu} = 0 \tag{4.13}$$

on $\partial\Omega \times (0, S)$. This equation is coupled to the heat equation (assuming without restriction of generality that $D = K = 1$)

$$\frac{\partial \theta}{\partial t} = \Delta \theta + \mathrm{e}^{-\varphi} \frac{\partial \varphi}{\partial t}, \qquad \theta|_{t=0} = \theta^0, \tag{4.14}$$

supplemented by the boundary condition (2.14). Thus, the underlying state equations are a parabolic and a hyperbolic equation with coupling in the source terms, which involve only lower-order derivatives with respect to time and space.

In this case we can choose the controls $q \in \mathcal{Q} = H^{2,1}(\partial\Omega \times (0, S))$ and the penalty term D as

$$D(r) := \frac{1}{2} \|r\|^2_{H^{2,1}(\partial\Omega \times (0,S))} \tag{4.15}$$

in the following. We note that $\mathcal{Q} \hookrightarrow H^{\frac{3}{2},\frac{3}{4}}(\partial\Omega \times (0, S))$, which implies that $\theta \in H^{2,1}(\Omega \times (0, S))$ and $\varphi \in H^{2,2}(\Omega \times (0, S))$ for sufficently regular domain Ω (cf. [25] for regularity results for evolution equations). For detailed results on the analysis of this system we refer to [2].

4.3. AVRAMI–KOLMOGOROV MODELS

The modelling approach by Avrami and Kolmogorov was used in its original form for spatially homogeneous crystallization (*cf.* [26, 27]), where the shape of the crystals is spherical until an

impingement effect occurs. In this case, the mean free-surface density u is determined by the equation

$$\frac{\partial u}{\partial t} = F(\theta), \qquad u(0) = 0, \tag{4.16}$$

with $F = 2\pi G\widetilde{N}$ as above. The relation (4.16) is frequently used for non-isothermal crystallization, too, coupled to the evolution equations (2.5), (2.6) (*cf.*, *e.g.*, [28, 29, 30]), where the growth of the crystal is computed as spherical growth driven by the growth rate for the temperature at the center of the spherulite. It can be shown that (4.16) is a scaling limit of (2.7), (2.8) for large nucleation rate and small growth rate (*cf.* [24, 13]); the physical interpretation of this approximation is that for small crystals the growth rate at the grain boundary and at the center do not differ significantly and the crystals cannot grow large due to the high number of nucleation events.

The state equations in the case of the generalized Avrami-Kolmogorov model can be rewritten in terms of the functions φ introduced in the previous sections together with the temperature θ and the mean surface density u, which yields (4.14) coupled to the second-order evolution equation

$$\frac{\partial \varphi}{\partial t} = G(\theta)u, \qquad \varphi|_{t=0} = 0, \tag{4.17}$$

$$\frac{\partial u}{\partial t} = F(\theta), \qquad u|_{t=0} = 0, \tag{4.18}$$

We want to mention that we can compute the functions φ and u as integrals of the temperature θ in this case, namely as

$$u(x,t) = \int_0^t F(\theta(x,s))\,\mathrm{d}s, \tag{4.19}$$

$$\varphi(x,t) = \int_0^t G(\theta(x,\tau)) \int_0^\tau F(\theta(x,s))\,\mathrm{d}s\,\mathrm{d}\tau. \tag{4.20}$$

As a direct consequence, the heat equation can be rewritten as an integro-differential equation, which simplifies the analysis. For numerical purposes the differential formulation of the Avrami-Kolmogorov model seems to be of advantage, since one can apply standard discretization methods for ODEs and parabolic PDEs. A simple, but nonetheless successful way to construct an efficient numerical scheme is to integrate the evolution equations for u and φ by an explicit method, before an implicit time step for the heat equation is performed. An alternative way is to discretize with respect to the spatial variable first and to apply integration methods (such as, *e.g.*, Runge-Kutta schemes) directly to the arising system of ODEs.

5. Solution of the spatially homogeneous problem

Now we turn our attention to the spatially homogeneous problem presented in the previous section. We shall discuss the existence of a minimizer as well as first-order optimality conditions and numerical methods for the solution of the problem.

5.1. Existence of a minimum

In the following we investigate the well-posedness of the state equation (4.3–4.6) and the solvability of the optimal-control problem (4.2–4.8).

Proposition 5.1. *Let F and G be Lipschitz-continuous and bounded on $\mathbb{R}$ and let $q \in Q_{ad}$. Then the initial-value problem (4.3–4.6) has a unique solution*

$$Z_q := (\gamma, \xi, u, \theta) \in C^1([0, S])^4. \tag{5.1}$$

Moreover, there exists a constant $c \in \mathbb{R}^+$, such that for all q_1 and q_2 in Q_{ad}, the estimate

$$\|Z_{q_1} - Z_{q_2}\|_{C^1([0,S)]} \leq c\|q_1 - q_2\|_{C([0,S)]}. \tag{5.2}$$

Proof. Under the above assumptions, the state equations (4.3–4.6) can be rewritten as an initial-value problem for the ordinary differential equation

$$\frac{\mathrm{d}Z_q}{\mathrm{d}t}(t) = R(Z_q, q), \qquad t \in [0, S],$$

where

$$R((\gamma, \xi, u, \theta), q) = \begin{pmatrix} G(\theta)(1-\xi)u^2 \\ G(\theta)(1-\xi)u \\ F(\theta) \\ \beta(\theta - q) + KG(\theta)(1-\xi)u \end{pmatrix},$$

where R is a Lipschitz-continuous function (and consequently continuous with respect to t, since $q \in C([0, S])$. Thus, the existence and uniqueness of a solution follows from the Picard-Lindelöf Theorem and (5.2) can be deduced in a straightforward way, noticing that R is Lipschitz-continuous with respect to q and that Q_{ad} is a bounded set in $C([0, S])$. □

The assumptions in Proposition 5.1 on the functions G and F are equivalent to the Lipschitz-continuity and boundedness of the material functions G and $\widetilde{N}$, which is fulfilled in typical models for these functions (*cf.* [11, 3]). Using the above well-posedness result for the state equation, we can also ensure the existence of a minimizer for (4.2), under the additional assumption that the inequality constraints (4.7) and (4.8) are consistent:

Theorem 5.2. *Let F and G be Lipschitz-continuous and bounded on $\mathbb{R}$ and assume that the admissible set of functions $(Z, q) \in C^1([0, S])^4 \times Q_{ad}$ satisfying (4.3–4.8) is nonempty. Then the optimal control problem (4.2–4.8) has a solution $(Z^*, q^*) \in C^1([0, S])^4 \times Q_{ad}$.*

Proof. Since the admissible set defined by (4.3–4.8) is compact in the space $C([0, S])^5$, there exists a sequence (Z_k, q_k) satisfying (4.3–4.8), which is convergent in $C([0, S])$ and such that

$$-\gamma_k(S) \to \inf(-\gamma(S)),$$

where the infimum is taken over all admissible points.

By standard techniques one can now show that the limit $(Z^*, q^*) \in C^1([0, S])^4 \times Q_{ad}$ is a solution of (4.3–4.6) and is still admissible. Since the functional $\gamma \mapsto -\gamma(S)$ is continuous on $C([0, S])$, we may conclude that

$$-\gamma^*(S) = \inf(-\gamma(S)),$$

i.e., (Z^*, q^*) is a solution of (4.2–4.8). □

5.2. First-order optimality

In the following we turn our attention to the first-order optimality conditions for (4.2–4.8), the so-called *Karush-Kuhn-Tucker system*. In the following we will always assume that F and G are continuously differentiable on $\mathbb{R}$, and we will use the notation $C_+([0, S])$ for the half-space

$$C_+([0, S]) := \{ \mu \in C([0, S]) \mid \mu(t) \geq 0, \forall\, t \in [0, S] \}. \tag{5.3}$$

It is well-known that the solution of an optimal control of the form (4.2–4.8) is also a saddle-point of the corresponding Lagrange functional $\mathcal{L}$ (*cf.* [31, 32]) defined by

$$\begin{aligned}\mathcal{L}(Z, q; P, M) := -\gamma(S) + \int_0^S P(t)^T \left(\frac{\mathrm{d}Z}{\mathrm{d}t}(t) - R(Z(t), q(t)) \right) \mathrm{d}t \\ + \int_0^S \left(\mu_1(t)(a + \frac{\mathrm{d}q}{\mathrm{d}t}) - \mu_2(t)\frac{\mathrm{d}q}{\mathrm{d}t} \right) \mathrm{d}t + \mu_3(\xi(S) - 1 + b),\end{aligned} \tag{5.4}$$

with $P = (\lambda_j)_{j=1,\dots,4} \in C([0, S])^4$, $M = (\mu_1, \mu_2, \mu_3) \in C_+([0, S])^2 \times \mathbb{R}^+$, *i.e.*,

$$\mathcal{L}(Z^*, q^*; P^*, M^*) = \inf_{(Z,q)} \sup_{(P,M)} \mathcal{L}(Z, q; P, M). \tag{5.5}$$

In this setup, P is the Lagrangian variable corresponding to the equality constraints (4.3–4.6), and M is the Lagrangian variable corresponding to the inequality constraints (4.7), (4.8).

The first-order optimality conditions can now be computed from the condition

$$\frac{\partial}{\partial(Z, q)} \mathcal{L}(Z^*, q^*; P^*, M^*)(Z - Z^*, q - q^*) \geq 0, \tag{5.6}$$

for all (Z, q) satisfying (4.7), (4.8).

We start this derivation from the partial derivatives with respect to the unconstrained variables γ, u and θ, for which equality holds in (5.6). After tedious calculation we obtain $\lambda_1^* \equiv 1$ and

$$0 = \frac{\mathrm{d}\lambda_3^*}{\mathrm{d}t} + G(\theta^*)(1 - \xi^*)(2u^* + \lambda_2^* + K\lambda_4^*), \tag{5.7}$$

$$0 = \frac{\mathrm{d}\lambda_4^*}{\mathrm{d}t} + G'(\theta^*)(1 - \xi^*)u^*(u^* + \lambda_2^* + K\lambda_4^*) + F'(\theta^*)\lambda_3^* + \beta\lambda_4^*, \tag{5.8}$$

supplemented by the terminal conditions $\lambda_3^*(S) = \lambda_4^*(S) = 0$.

For the optimality with respect to ξ, the situation is more difficult; here we obtain that

$$0 = \frac{\mathrm{d}\lambda_2^*}{\mathrm{d}t} - G(\theta^*)u^*(u^* + \lambda_2^* + K\lambda_4^*), \tag{5.9}$$

supplemented by the terminal condition $\lambda_2^*(S) = \mu_3^*$. If $\xi(S) \neq 1 - b$, where the according Lagrange multiplier μ_3^* equals zero and we conclude that $\lambda_2^*(S) = 0$.

Finally, we derive the optimality condition with respect to the control q, which yields a differential equation for the Lagrange-parameters μ_1 and μ_2, namely

$$\frac{\mathrm{d}}{\mathrm{d}t}(\mu_1^* - \mu_2^*) = \beta\lambda_4^*, \qquad \mu_1^*(S) = \mu_2^*(S). \tag{5.10}$$

5.3. Structure of the solution: a bang-bang principle

In the following we investigate the structure of a stationary point, i.e., a state Z^*, a control q^* and according Lagrange variables satisfying the first-order optimality conditions deduced in the previous section. To this end we assume that F and G are nonnegative functions which are monotonely non-increasing in the temperature range of interest.

A first observation is that the difference between the Lagrange variables μ_1 and μ_2 satisfies

$$\mu_1^*(t) - \mu_2^*(t) = \int_S^t \beta\lambda_4^*(s)\,\mathrm{d}s, \tag{5.11}$$

which follows from (5.10). Together with the nonnegativity of the Lagrange variables and the complementarity conditions

$$\mu_1^*(t)\left(a + \frac{\mathrm{d}q^*}{\mathrm{d}t}(t)\right) = \mu_2^*(t)\frac{\mathrm{d}q^*}{\mathrm{d}t}(t) = 0, \tag{5.12}$$

this implies a bang-bang principle for the solution, *i.e.*, for almost all $t \in (0, S)$ we either have $\frac{\mathrm{d}q}{\mathrm{d}t}(t) = -a$, $\frac{\mathrm{d}q}{\mathrm{d}t}(t) = 0$ or the integral on the right-hand side of (5.11) vanishes.

For some special cases we will show in the following that the third case cannot occur on an open time interval and thus, an optimal cooling strategy is a combination of time intervals with either maximal cooling or temperature kept fixed.

5.4. Special cases

In the following we examine some special cases that provide further insight into the optimal-control problem and the structure of its solutions.

5.4.1. *Averaged growth*

In the following we assume that G is constant and F is a nonnegative, continuously differentiable function, which allows some further investigations on the structure of optimal controls.

Suppose that the right-hand side in (5.11) is identical zero in a time interval (t_1, t_2), which is only possible if $\lambda_4^* \equiv 0$ in (t_1, t_2). Then (5.8) reduces to $F'(\theta^*)\lambda_3^* = 0$ and, thus, we either have that $\lambda_3^* \equiv 0$ or $F'(\theta^*) \equiv 0$ on an open subinterval of (t_1, t_2). We shall examine these two cases in the following; without restriction of generality we assume that this subinterval coincides with (t_1, t_2).

If we assume that the nucleation rate is constant below the glass-transition temperature and above the melting point, then $F'(\theta^*) = 0$ occurs in these two temperature regions. If we assume that F has a single extremal point (a maximum) in this temperature range, then the only other case where $F'(\theta^*) = 0$ occurs if the temperature is kept constant at this maximizing value.

If $\lambda_3^* \equiv 0$, we may deduce together with (5.7) that $\lambda_2^* = -2u^*$ in (t_1, t_2) and (5.9) implies that

$$\frac{\mathrm{d}u^*}{\mathrm{d}t}(t) = \frac{G}{2}u^*(t)^2.$$

Hence, we obtain that either $u^* \equiv 0$ in (t_1, t_2) or $u^*(t) = (c - Gt)^{-1}$ for some positive real number $c > Gt_2$. Together with the evolution equation for u^* this yields that

$$F(\theta^*) = \frac{\mathrm{d}u^*}{\mathrm{d}t} = \frac{G}{2}u^*(t)^2 = \frac{G}{2(c - Gt)^2},$$

which implies that

$$\theta^* = F^{-1}\left(\frac{G}{2(c-Gt)^2}\right),$$

where F^{-1} is the inverse function of F in the temperature range occuring in (t_1, t_2), which exists because we have excluded the possibility of $F'(\theta^*) = 0$ here. Moreover, we can compute the degree of crystallinity in this time interval via

$$\xi^*(t) = 1 - d_0 \mathrm{e}^{-G\int_{t_1}^t u^*(s)\,\mathrm{d}s} = 1 - d_0\frac{c-Gt}{c-Gt_1} = 1 - d(c-Gt)$$

for some positive real number d_0 and $d = d_0(c - Gt_1)^{-1} > 0$. This means that the degree of crystallinity grows with constant speed dG in this time interval.

Thus, we have identified five different possibilities, one of which an optimal control must satisfy:

1. The temperature is kept below the melting point in an initial time interval, which implies that $F(\theta^*) = 0$ and, thus, the crystallization starts with some delay. The occurence of this case gives evidence that the final time S is chosen too large and can be reduced by the length of the initial time interval without any consequences for the result;
2. The temperature is kept below the glass-transition temperature for some time interval, which implies that no further crystallization occurs;
3. The temperature is kept constant at the maximizing value of the nucleation rate for some time interval;
4. One of the constraints on the control is active, *i.e.*, either $\frac{\mathrm{d}q}{\mathrm{d}t} = 0$ or $\frac{\mathrm{d}q}{\mathrm{d}t} = -a$;
5. The degree of crystallinity grows with constant speed (proportional to G) over some time interval.

5.4.2. *Strong asymptotics*

Below we obtain the spatially homogeneous case as a limit of the three-dimensional case if the height of the sample is sufficiently small. Since this height is proportional to β^{-1}, we may expect β to be very large compared to other parameters. If we have, in particular, that $\beta \gg 1$ and $\beta \gg KG$, the re-heating effect in the heat equation is negligible and the control variable q is a good approximation for the temperature θ. Since $q(0) = \theta(0)$, there is also no initial time layer with bad approximation properties as one usually would obtain for $\beta^{-1} \to 0$. Thus, it seems reasonable to eliminate the state equation for the temperature and to act directly on the temperature as the control variable, which yields the new state equation

$$\frac{\mathrm{d}}{\mathrm{d}t}\begin{pmatrix}\gamma\\ \xi\\ u\end{pmatrix} = \begin{pmatrix}G(\theta)(1-\xi)u^2\\ G(\theta)(1-\xi)u\\ F(\theta)\end{pmatrix}.$$

In an analogous way to the computations above we can also derive first-order optimality conditions in this case, now for a reduced set of Lagrange parameters $(\lambda_1, \lambda_2, \lambda_3; \mu_1, \mu_2, \mu_3)$. The optimality conditions for λ_i lead again to $\lambda_1^* \equiv 1$ and

$$\frac{\mathrm{d}}{\mathrm{d}t}\begin{pmatrix}\lambda_2^*\\ \lambda_3^*\end{pmatrix} = \begin{pmatrix}G(\theta^*)u^*(u^*+\lambda_2^*)\\ -G(\theta^*)(1-\xi^*)(2u^*+\lambda_2^*)\end{pmatrix}.$$

The Lagrange-parameters μ_1 and μ_2 satisfy the complementary conditions and the equation

$$\frac{\mathrm{d}}{\mathrm{d}t}(\mu_1^* - \mu_2^*) = -G'(\theta^*)(1-\xi^*)u^*(u^*+\lambda_2^*) - F'(\theta^*)\lambda_3^*, \quad \mu_1^*(S) = \mu_2^*(S),$$

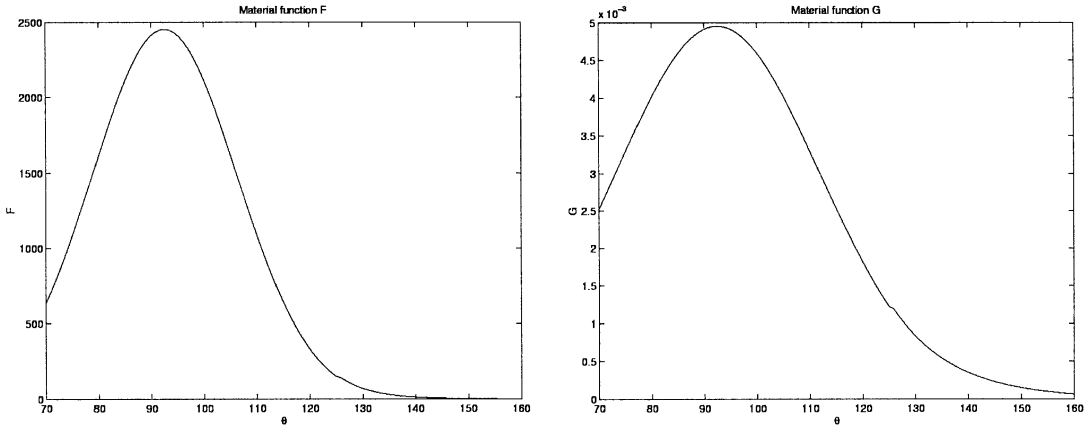

Figure 2. Plot of the material functions F (above) and G (below) *vs.* temperature.

the condition for μ_3 remains unchanged to the general case.

We want to mention that for constant growth rate G, an analogous reasoning as in the general case is possible, which reduces the behavior of optimal controls again to five cases.

6. Numerical experiments

For our numerical experiments we investigate the spatially homogeneous problem, first in the strong asymptotic case $\beta^{-1} = 0$ and then in the general case, which permits re-heating and therefore yields a more complex problem.

The parameters used in the model are oriented on the values for isotactic polypropylene (i-PP), which can be found, *e.g.*, in [13]. The constraint on the cooling temperature is given by $a = 0{\cdot}5$ K per second (except in one example with $a = 2\ \mathrm{Ks}^{-1}$), which is a typical cooling speed in polymer processing. The parameter for the state constraint was chosen as $b = 0{\cdot}1$ and the processing time was $S = 3$ minutes. The material functions F and G we used for our computations are shown in Figure 6.

The problem is solved numerically by performing first an implicit time discretization and by applying a sequential quadratic programming-type method to the ensuing finite-dimensional system of equations. All computations have been performed using the software system MATLAB, the optimization algorithm was taken from the MATLAB Optimization Toolbox.

6.1. Solution for $\beta^{-1} = 0$

In this special case we have performed a numerical test starting from the uniform initial temperature $q \equiv T_m$ and the corresponding degree of crystallinity $\xi \equiv 0$ and the surface density $u \equiv 0$. This initial value is non-feasible in the sense that it does not satisfy the state constraint, but this is not required by the optimization algorithm we use.

The optimization algorithm computed an optimal solution with final density $\gamma^*(S) = 2{\cdot}28 \times 10^8$. The resulting optimal control q^* is plotted on the left side of Figure 6.1, from which one observes that maximal cooling is optimal in almost the whole time interval. This numerical result is not really surprising, since the re-heating effect is not present in this test case and the cooling speed is not extremely high (so that the temperature is always below the maximum of the material functions). The evolution of the degree of crystallinity and of

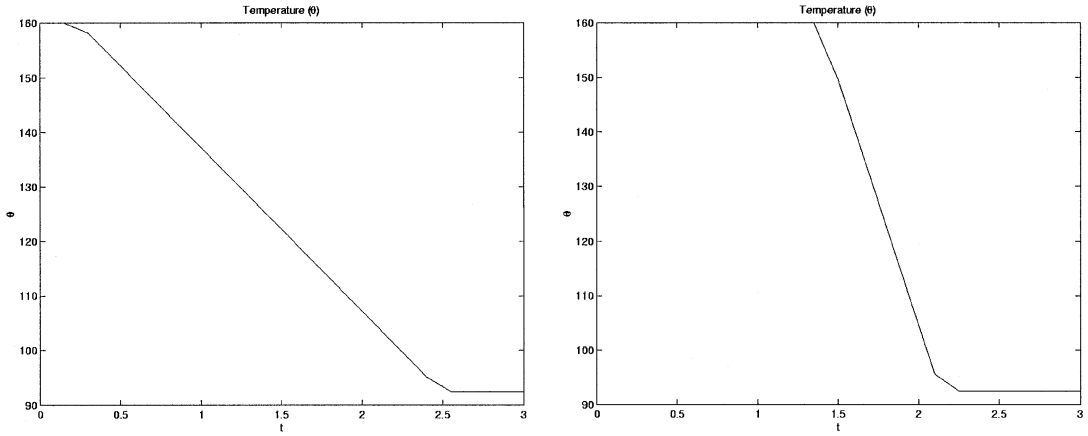

Figure 3. Optimal cooling temperature $q^* = \theta^*$ for $a = 0{\cdot}5\ \mathrm{Ks}^{-1}$ (above) and for $a = 2\ \mathrm{Ks}^{-1}$ (below).

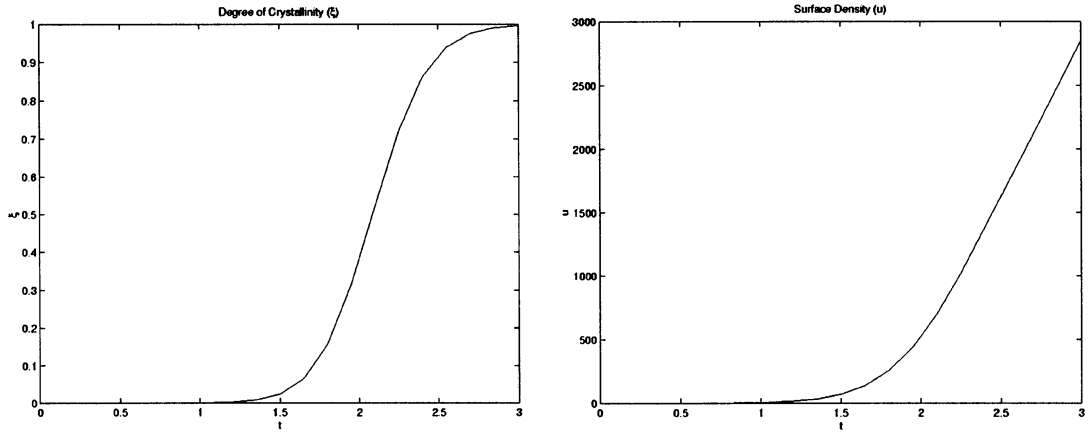

Figure 4. Evolution of crystallinity ξ^* and surface density u^* for $a = 0{\cdot}5\ \mathrm{Ks}^{-1}$.

the surface density are shown in Figure 6.1; as usual most crystals are produced and grow in medium time interval.

For an increased cooling speed (to $a = 2\ \mathrm{Ks}^{-1}$), the situation is slightly different, as one observes in the right plot in Figure 6.1 and in Figure 6.1, where the optimal cooling strategy and the corresponding evolution of crystallinity and surface density are shown. In this case, the optimal control is obtained by (almost) maximal cooling only in the second half of the time interval, a further temperature increase does not yield a higher contact-interface density, since the material is completely crystallized. An interesting consequence of this result is that the processing time could be reduced significantly with the same quality of the final product. The (negative) objective value in this case is $\gamma^*(S) = 2.94 \times 10^8$, which is not much larger than in the previous case with slower cooling.

6.2. Solution in the general case

In the general case we consider two different numerical examples illustrating the effect of the latent heat, which represents the essential difference with the strongly asymptotic case investigated above. In the first case we chose $\beta = -10^4$ and $K = 1K$, which corresponds to

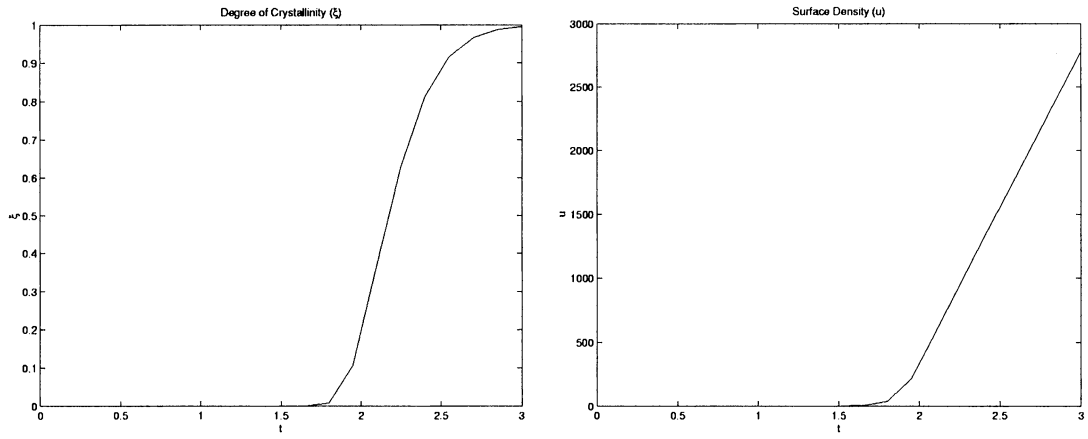

Figure 5. Evolution of crystallinity ξ^* and surface density u^* for $a = 2\ \mathrm{Ks}^{-1}$.

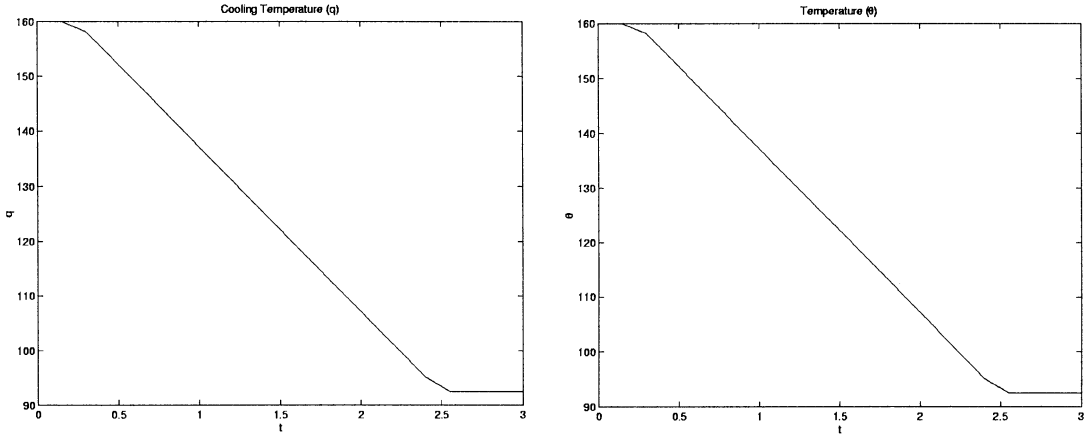

Figure 6. Optimal cooling strategy q^* and evolution of the temperature θ^* for $\beta = -10^4$; $K = 1$.

a rather low latent heat, while the second example was carried out with the parameter settings $\beta = -10^3$ and $K = 100K$. In both cases we chose $a = 0{\cdot}5\ \mathrm{Ks}^{-1}$, $b = 0{\cdot}1$ $S = 3$ minutes, *i.e.*, in the same way as in the first example above.

The optimal controls q^* determined in the first case and the corresponding temperature evolutions θ^* are plotted in Figure 6.2. One observes that in this case the solution does not differ much from the one obtained for $\beta^{-1} = 0$, *i.e.*, it seems that the parameters are close enough to the asymptotics such that one could obtain a reasonable result with the reduced model used in the examples above. This is also reflected by the objective value $\gamma^*(S) = 2{\cdot}28 \times 10^8$, which is almost the same as for $\beta^{-1} = 0$. The effect of latent heat is still very small compared to the effect of the small sample height leading to a large value of β. A comparison of the cooling temperature q^* and the effective temperature θ^* shows even more clearly that the difference is almost neglible. The evolution of the degree of crystallinity ξ^* and of the surface density u^* are shown in Figure 6.2.

Not surprisingly, the situation differs in the second case, *i.e.*, for smaller β $(= 10^3)$ and larger latent heat ($K = 100$ K), which can be observed from Figures 6.1 and 7. The optimal cooling is now slower than in the previous case and the resulting temperature evolution shows significant differences in the cooling temperature. In addition, one clearly observes the re-

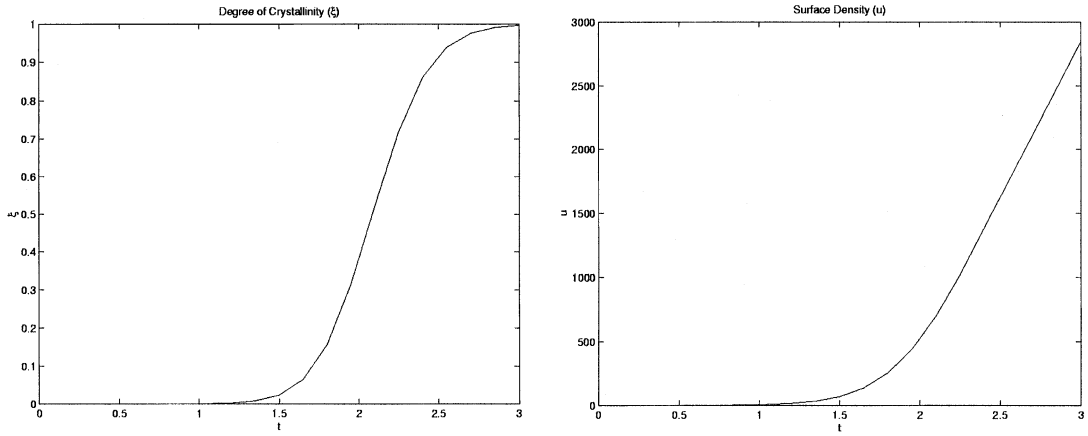

Figure 7. Evolution of crystallinity ξ^* and surface density u^* for $\beta = -10^4$; $K = 1$.

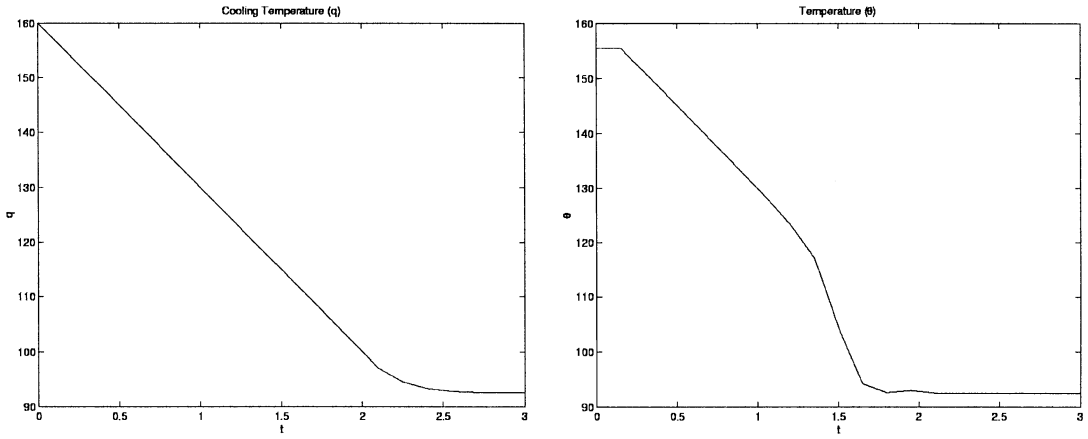

Figure 8. Optimal cooling strategy q^* and evolution of the temperature θ^* for $\beta = -10^3$; $K = 10^2$.

heating effects due to the release of latent heat in the plot of θ^* in Figure 6.2. The objective value in this case is $\gamma^*(S) = 2{\cdot}77 \times 10^8$, which is larger than for low latent heat, *i.e.*, the re-heating effect supports fine grained structures.

7. Concluding remarks

We have formulated a rather general optimal control problem for the purpose of obtaining materials of optimal structure by controlling the cooling temperature during the solidification process. In the most general case, our approach yields an optimal-control problem for a system of time-dependent partial differential equations in three spatial dimensions, whose (challenging) numerical solution we leave to future research.

Because of their practical importance and in order to obtain further insight into the optimal-control problem, we have discussed several special cases, some of them leading to optimal-control problems for systems of ordinary differential equations. An investigation of the corresponding optimality system showed that the optimal solution must satisfy a bang-bang principle, which implies that the optimal cooling strategy is a combination of five different simple strategies.

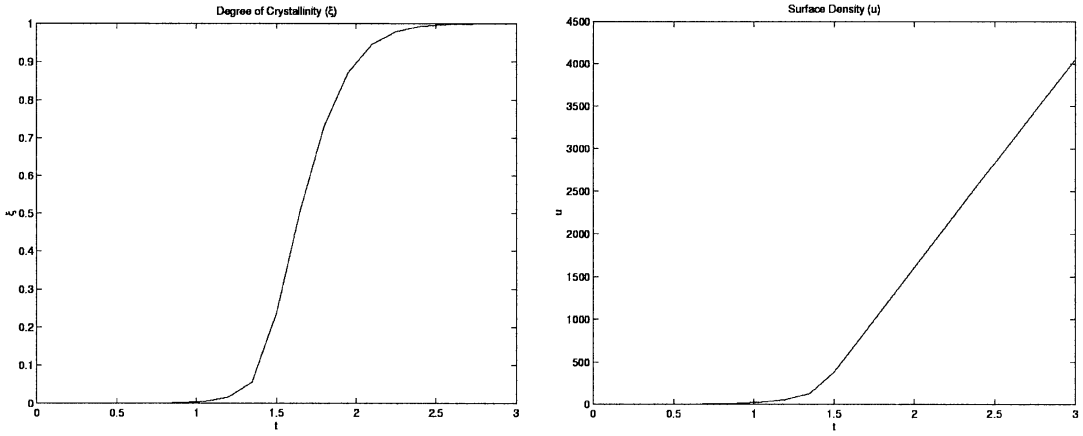

Figure 9. Evolution of crystallinity ξ^* and surface density u^* for $\beta = -10^3$; $K = 10^2$.

The theoretical results are supported by numerical experiments carried out for special cases, which exhibit the bang-bang type structure of the optimal control. Moreover, the numerical results give further insight in the behaviour of the solution regarding its dependence on some material and process parameters such as the latent heat and the maximum cooling speed.

Acknowledgements

Financial support by the EU is acknowledged under the TMR-Network *Differential Equations in Industry and Commerce* (M.B.,V.C.,A.M.), by the Austrian Science Foundation under project SFB F 13/08 (M.B.) by the Italian MURST/cofin. Programme "Stochastic Processes with Spatial Structure"(V.C.,A.M.), and by the Italian CNR contract n. 98.03635.ST74 (V.C.,A.M.).

References

1. V. Capasso, ed., *Mathematical Modelling for Polymer Processing. Polymerization, Crystallization, Manufacturing*. Heidelberg: Springer (2002) 320 pp.
2. M. Burger, Iterative regularization of an identification problem arising in polymer crystallization. *SIAM J. Num. Anal.* 39 (2001) 1029–1055.
3. M. Burger, V. Capasso and H.W. Engl, Inverse problems related to crystallization of polymers. *Inverse Problems* 15 (1999) 155–173.
4. E. Ratajski and H. Janeschitz-Kriegl, How to determine high growth speeds in polymer crystallization. *Colloid Polymer Sci.* 274 (1996) 938–951.
5. P. Supaphol and J.E. Spruiell, Thermal properties and isothermal crystallization of syndiodactic polypropylenes: differential scanning calorimetry and overall crystallization kinetics. *J. Appl. Polymer Sci.* 75 (2000) 44–59.
6. D.C. Bassett, *Principles of Polymer Morphology.* Cambridge: Cambridge University Press (1981) 251 pp.
7. D.W. Van Krevelen, *Properties of Polymers.* Amsterdam: Elsevier (1990) 875 pp.
8. L.H. Friedman and D.C. Chrzan, Scaling theory of the Hall-Petch relation for multilayers. *Phys. Rev. Lett.* 81 (1998) 2715–2719.
9. M. Burger, V. Capasso and C. Salani, Modelling multi-dimensional crystallization of polymers in interaction with heat transfer. *Nonlin. Anal. Real World Applic.* 3 (2002) 139–160.

10. V. Capasso and C. Salani, Stochastic birth-and-growth processes modelling crystallization of polymers in a spatially heterogenous temperature field. *Nonlin. Anal. Real World Applic.* 1 (2000) 485–498.
11. M. Burger, V. Capasso and G. Eder, Modelling crystallization of polymers in temperature fields. *Zeitschrift Angew. Math. Mech.* 82 (2002) 51–63.
12. B. Monasse and J.M. Haudin, Thermal dependence of nucleation and growth rate in polypropylene by non-isothermal calorimetry. *Colloid Polymer Sci.* 264 (1986) 117–122.
13. M. Burger and V. Capasso, Mathematical modelling and simulation of non-isothermal crystallization of polymers. *Math. Models Methods Appl. Sci.* 11 (2001) 1029–1053.
14. A. Friedman and J.L. Velazquez, A free boundary problem associated with crystallization of polymers in a temperature field. *Indiana Univ. Math. J.* 50 (2001) 1609–1649.
15. V. Capasso, A. Micheletti and G. Eder, Polymer crystallization processes and incomplete Johnson-Mehl tesselations. In: L. Arkeryd, J. Bergh, P. Brenner and R. Pettersson (eds), *Progress in Industrial Mathematics at ECMI 98.* Stuttgart, Leipzig: Teubner (1999) pp. 130–137.
16. S.N. Chiu, Limit theorems for the time of completion of Johnson-Mehl tessellations. *Adv. Appl. Prob.* 27 (1995) 889–910.
17. A. Micheletti and V. Capasso, The stochastic geometry of polymer crystallization processes. *Stoch. Anal. Applic.* 15 (1997) 355–373.
18. J. Moeller, Random Johnson-Mehl tessellations. *Adv. Appl. Prob.* 24 (1992) 814–844.
19. J. Moeller, Generation of Johnson-Mehl crystals and comparative analysis of models for random nucleation. *Adv. Appl. Prob.* 27 (1995) 367–383.
20. V. Capasso and A. Micheletti, Local spherical contact distribution function and local mean densities for inhomogeneous random sets. *Stochastics Stochastics Reports* 71 (2000) 51–67.
21. V. Capasso, A. Micheletti and M. Burger, Densities of n-facets of incomplete Johnson-Mehl tessellations generated by inhomogeneous birth-and-growth processes. Quaderno del Dipartimento di Matematica, Universita di Milano 38 (2001).
22. R.A. Adams. *Sobolev Spaces.* New York: Academic Press (1975) 268 pp.
23. L.C. Evans, *Partial Differential Equations.* Providence: AMS (1998) 662 pp.
24. M. Burger, *Direct and Inverse Problems in Polymer Crystallization Processes.* Linz: PhD-Thesis, University Linz (2000) 157 pp.
25. J.L. Lions and E. Magenes, *Non-Homogenous Boundary Value Problems and Applications, Volume II.* Berlin, Heidelberg, New York: Springer (1972) 242 pp.
26. M. Avrami, Kinetics of phase change I-III. *J. Chem. Phys.* 7 (1939) 1103–1112; 8 (1940) 212–224; 9 (1941) 177–184.
27. A.N. Kolmogorov, On the statistical theory of the crystallization of metals. *Bull. Acad. Sci. USSR, Math. Series* 1 (1937) 355–359.
28. G. Eder, Crystallization kinetic equations incorporating surface and bulk nucleation. *Zeitschrift Angew. Math. Mech.* 76 (1996) S4, 489–492.
29. G. Eder, Fundamentals of structure formation in crystallizing polymers. In: K. Hatada, T. Kitayama and O. Vogl (eds), *Macromolecular Design of Polymeric Materials.* New York: Marcel Dekker (1997) pp. 761–782.
30. W. Schneider, A. Köppl and J. Berger, Non-isothermal crystallization. Crystallization of polymers. *Int. Polymer Processing* 2 (1988) 151–154.
31. R.V. Gamkrelidze, *Principles of Optimal Control Theory.* New York, London: Plenum Press (1978) 175 pp.
32. G. Knowles, *An Introduction to Applied Optimal Control.* New York: Academic Press (1981) 180 pp.